Columnar Metallomesogens Derived from 1,3,4-Oxadiazoles and X-ray Crystal Structure of Dichlorobis[2,5-bis(3,4,5-trimethoxyphenyl)-1,3,4-oxadiazole]palladium(II)

Chang-Rong Wen,[†] Yueh-Ju Wang,[†] Hsiang-Cheng Wang,[†] Hwo-Shuenn Sheu,[‡] Gene-Hsiang Lee,[§] and Chung K. Lai*,[†]

Department of Chemistry, National Central University, Chung-Li, Taiwan 32054, ROC and Center for Nano Science and Technology, University System of Taiwan, National Synchrotron Radiation Research Center, Hsinchu 30077, Taiwan, ROC, and Instrumentation Center, National Taiwan University, Taipei 10660, Taiwan, ROC

Received September 19, 2004. Revised Manuscript Received January 14, 2005

Three series of palladium(II) complexes **1**−**3** derived from 1,3,4-oxadiazoles exhibiting mesogenic properties are prepared and characterized. It was found that the formation of mesophases was sensitive to the numbers of alkoxy side chains. The compounds **3** appended with twelve side chains exhibited columnar (Col) phases, however, all other compounds **1**−**3** appended with four or eight side chains formed crystalline phases. Some derivatives ($n = 8$, 10, 12) of the series **3** were in fact mesogenic at room temperature. Powder XRD data indicated that the formation of columnar mesophase varied from rectangular (Col_r) to hexagonal arrangements (Col_h) was observed as carbon chains length increases. The crystal and molecular structure of palladium(II) complex of 2,5-bis(3,4,5-trimethoxy phenyl)-1,3,4-oxadiazole (**3**; $n = 1$) was determined by means of X-ray structural analysis. It crystallizes in the monoclinic space group $p2_1/n$, with $a = 8.7736$ (3) Å, $b = 19.1568$ (6) Å, $c = 15.7834$ (5) Å, $\beta = 100.106$ (1)°, and $Z = 2$. The geometry at palladium center is perfectly square planar, and two *trans*-chlorine atoms are almost perpendicularly located to the molecular plane determined by four 1,3,4-oxadiazole rings. The fluorescent properties of these compounds were also examined. All λ_{max} peaks of the absorption and photoluminescence spectra of compounds **4** and **6** occurred at ca. 303−312 nm and 358−391 nm, respectively; whereas the quantum yields of some compounds were relatively low.

Introduction

Heterocyclic oxadiazoles have been extensively studied for a long time due to their high thermal and hydrolytic stability.[1] Most work has concentrated on the symmetric 1,2,5- and 1,3,4-oxadiazoles, and considerably less work has been focused on the nonsymmetric 1,2,4-oxadiazoles. A variety of 1,2,4-oxadiazole derivatives have been reported to show a wide range of interesting biological activities.[2] A few examples of oxadiazole-based compounds have been recently used as electron transport materials[3] in organic ligh-emitting diodes (OLEDs). The novel optical or/and electrical properties exhibited by such cores were mainly attributed to their electron deficiency, high photoluminescence quantum yields, and good thermal and chemical stabilities of the oxadiazole ring.

1,3,4-Oxadiazole derivatives were considered nonlinear mesogenic compounds.[4] Utilization of such a heterocyclic ring in which the molecular symmetry of the central core is reduced would possibly lead to a lowering of melting points due to a less favorably packing in the crystal state.[5] The physical behavior[6] was focused on electron-transporting capability or photoconducting for advanced electronic devices. Nonmesomorphic 2,5-bis(4-naphthyl)-1,3,4-oxadiazole[7] was found as one of the best organic electron

* To whom correspondence should be addressed. E-mail: cklai@cc.ncu.edu.tw.
[†] National Central University, and Center for Nano Science and Technology, UST.
[‡] National Synchrotron Radiation Research Center.
[§] National Taiwan University.

(1) (a) Collins, I. *J. Chem. Soc., Perkin Trans.* **2000**, *1*, 2845. (b) Warkentin, J. *J. Chem. Soc., Perkin Trans.* **2000**, *1*, 2161. (c) Schulz, B.; Bruma, M.; Brehmer, L. *Adv. Mater.* **1997**, *9*, 601.
(2) (a) Buscemi, S.; Vivona, N. *J. Org. Chem.* **1996**, *61*, 8397. (b) Cerecetto, H.; Di Maio, R.; González, M.; Risso, M.; Saenz, P.; Seoane, G.; Denicola, A.; Peluffo, G.; Quijano, C.; Olea-Azar, C. *J. Med. Chem.* **1999**, 1941. (c) Shi, W.; Qian, X.; Zhang, R.; Song, G. *J. Agric. Food Chem.* **2001**, *49*, 124.
(3) (a) Zheng, Y.; Lin, J.; Liang, Y.; Lin, Q.; Yu, Y.; Meng, Q.; Zhou, Y.; Wang, S.; Wang, H.; Zhang, H. *J. Mater. Chem.* **2001**, *11*, 2615. (b) Sano, T.; Nishio, Y.; Hamada, Y.; Takahashi, H.; Usuki, T.; Shibata, K. *J. Mater. Chem.* **2000**, *10*, 157. (c) Noda, T.; Ogawa, H.; Noma, N.; Shirota, Y. *J. Mater. Chem.* **1999**, *9*, 2177. (d) Jiang, X.; Liu, Y.; Tian, H.; Qiu, W.; Song, X.; Zhua, D. *J. Mater. Chem.* **1997**, *7*, 1395. (e) Carella, A.; Castaldo, A.; Centore, R.; Fort, A.; Sirigu, A.; Tuzi, A. *J. Chem. Soc., Perkin Trans.* **2002**, *2*, 1791. (f) Wang, J.; Wang, R.; Yang, J.; Zheng, Z.; Carducci, M. D.; Cayou, T. *J. Am. Chem. Soc.* **2001**, *123*, 6179.
(4) Dingemans, T. J.; Samulski, E. T. *Liq. Cryst.* **2000**, *27*, 131.
(5) Lai, L. L.; Wang, C. H.; Hsieh, W. P.; Lin, H. C. *Mol. Cryst. Liq. Cryst.* **1996**, *287*, 177.
(6) (a) Cha, S. W.; Choi, S. H.; Kim, K.; Jin, J. I. *J. Mater. Chem.* **2003**, *13*, 1900. (b) Wang, C.; Jung, G. Y.; Batsanov, A. S.; Bryce, M. R.; Petty, M. C. *J. Mater. Chem.* **2002**, *12*, 173. (c) Adachi, C.; Tsutsui, T.; Saito, S. *Appl. Phys. Lett.* **1989**, *55*, 1489. (d) Hamada, Y.; Adachi, C.; Tsutsui, T.; Saito, S. *Jpn. J. Appl. Phys.* **1992**, *31*, 1812. (e) Wagner, H. J.; Loutfy, R. O.; Hsiao, C. K. *J. Mater. Sci.* **1982**, *17*, 2781. (f) Closs, F.; Siemensmeyer, K.; Frey, K.; Funhoff, D. *Liq. Cryst.* **1993**, *14*, 629. (g) Kaminorz, Y.; Schulz, B.; Brehmer, L. *Synth. Met.* **2000**, *111*, 75. (h) Giebler, R.; Schulz, B.; Reiche, J.; Brehmer, L.; Wühn, M.; Wöll, Ch.; Smith, A. P.; Urquhart, S. G.; Ade, H. W.; Unger, W. E. S. *Langmuir* **1999**, *15*, 1291.

10.1021/cm0483691 CCC: $30.25
Published on Web 03/05/2005

conductors. On the other hand, examples of mesomorphic 1,3,4-oxadiazole[8] or 1,3,4-thiadiazole[9] derivatives were relatively scarce, and most of them were generally rodlike molecules[8] exhibiting nematic/smectic phases. For example, 2,5-bis(4-octadecyloxybenzylidene-4-aminophenyl)-1,3,4-oxadiazole[10] exhibited nematic/smectic phases and also possessed electron-transporting capability. In contrast, columnar 1,3,4-oxaziazole derivatives[11,12] were relatively limited. A star-shaped discotic molecule containing 1,3,5-triethynylbezene and oxadiazole-based rigid arms was reported[11] to exhibit a discotic nematic phase (N_{Col}). A reduced intercore interaction caused by the nonplanar oxadiazole ring was believed to be responsible for the formation in this type of discotic nematic phase.

A new series of 1,3,4-oxadiazole-based compounds, 2,5-bis(3,4,5-trialkoxyphenyl)-1,3,4-oxadiazoles that exhibited hexagonal columnar phases (Col_h) were reported in our previous paper,[12] and most of them were in fact room-temperature liquid crystals. On the other hand, the two heteroatoms such as N and O with free electron pairs on the five-member rings could provide active potential coordination site for metal ions. Nonmesogenic metal complexes[13] such as Ag, Ru, or Cu were long known, however, mesogenic metal complexes derived from 1,3,4-oxadiazoles still remained unknown.

In this work, as part of our continuing research in metallomesogens we describe herein the preparation and mesomorphic studies of a new series of palladium(II) complexes derived from symmetric 1,3,4-oxadiazole core. These palladium(II) complexes exhibit columnar phases, and some of these compounds **3** (n = 8, 10, 12) are room-temperature liquid crystals. To our knowledge, this is the first metal complex derived from 1,3,4-oxadiazole that exhibited columnar phases.

Results and Discussion

Synthesis and Characterization. Two synthetic routes[12,14] in preparing 1,3,4-oxadiazole derivatives via intermediate tetrazoles or hydrazides were long known. The synthetic procedures used to prepare compounds **1**−**3** in this work are given in Scheme 1. The 1,3,4-oxadiazole derivatives were similarly prepared by our previous procedures, and all these derivatives were obtained by condensation reaction of hydrazides and PCl_3 in refluxing dried toluene. Formation of an orange jello-like paste as side product was observed in the reaction, which is probably due to possible polymerization leading to a lower yield. However, the side reaction is easily reduced to a minimum by controlling the reaction time to less than 8 h. All derivatives were isolated as white solids or pastes depending on the carbon length attached. All compounds were characterized by ^{1}H NMR and ^{13}C NMR spectroscopy. Palladium complexes were obtained by reactions of 2,5-bis(3,4,5-trialkoxyphenyl)-1,3,4-oxadiazoles and palladium(II) chloride in refluxing C_2H_5OH/H_2O for 24 h. The products were generally recrystallized from CH_2Cl_2/CH_3OH and isolated as yellow solids with a yield range 80−91%. The complexes were also characterized by FT-IR spectroscopy and elemental analysis.

Single-Crystal Structure of Dichloro-bis[2,5-bis(3,4,5-trimethoxyphenyl)-1,3,4-oxadiazole]palladium(II) Complex (3, n = 1). The crystal structure of the nonmesogenic Pd complex was investigated. Light yellow platelike crystals suitable for X-ray diffraction analysis were obtained from slowly grown CH_2Cl_2 solution at room temperature. Figure 1 shows the molecular structure with the atomic numbering scheme. The geometry at palladium center is a perfect square planar. The two angles of N(1)−Pd−Cl(1) and N(1)−Pd−Cl(1a) are 89.06(6)° and 90.94(6)°, respectively, which show almost an ideal angle of 90° as expected for a square-planar geometry. The overall molecular shape is nearly flat, and the two *trans*-chlorine atoms are located perpendicular to the molecular plane determined by four 1,3,4-oxadiazole rings. The bond lengths of two Pd−Cl and Pd−N bonds are equally of 2.3062(6) Å and 2.0063(19) Å. The overall length and the width of the molecule are estimated ca. 14.47 Å and 13.39 Å, which are ideally expected for a round molecule. Two different views of the crystal packing in the unit cell are presented in Figure 2, and reveal that the molecules are packed in a slight tilt arrangement within the columns. The perpendicular distance between the two heterocyclic 1,3,4-oxadiazole rings in neighboring molecules is estimated ca. 4.161 Å, and the distance between the two chlorines on the same side of molecular plane in neighboring molecules is also estimated ca. 8.216 Å. This molecular arrangement is quite consistent with the rectangular columnar phases observed by powder XRD and optical textures.

Mesomorphic Properties and Powder XRD Data. The compounds **4**−**6** were previously prepared[12] and their mesomorphic properties were also investigated by this group. The mesomorphic results indicated that all the compounds **6** (n = 5, 6, 7, 8, 10, 12, 14, 16) exhibited hexagonal columnar (Col_h) phases, and some derivatives (n = 6, 7, 8, 10) were room-temperature liquid crystals. However, all other similar compounds **4**−**5** with fewer side chains formed crystalline phases. To understand the relationship between the molecular structures and the phase properties, the palladium complexes with various numbers of alkoxy side chains were prepared and their thermal properties were investigated. All palla-

(7) Tokuhisa, H.; Era, M.; Tsutsui, T.; Saito, S. *Appl. Phys. Lett.* **1995**, *66*, 3433.
(8) (a) Karamysheva, L. A.; Torgova, S. I.; Agafonova, I. F.; Petrov, V. F. *Liq. Cryst.* **2000**, *27*, 393. (b) Semmler, K. J. K.; Dingemans, T. J.; Samulski, E. T. *Liq. Cryst.* **1998**, *24*, 799. (c) Hetzheim, A.; Wasner, C.; Werner, J.; Kresse, N.; Tschierske, C. *Liq. Cryst*. **2000**, *26*, 885.
(9) (a) Parra, M.; Alderete, J.; Zuñiga, C.; Jimenez, V.; Hidalgo, P. *Liq. Cryst*. **2003**, *30*, 297. (b) Xu, Y.; Li, B.; Liu, H.; Guo, Z.; Tai, Z.; Xu, Z. *Liq. Cryst*. **2002**, *29*, 199. (c) Parra, M.; Hernández, S.; Alderete, J.; Zu, C. *Liq. Cryst*. **2000**, *27*, 995.
(10) Tokuhisa, H.; Era, M.; Tsutsui, T. *Chem. Lett.* **1997**, 303.
(11) Kim, B. G.; Kim, S.; Park, S. Y. *Tetrahedron Lett.* **2001**, *42*, 2697.
(12) Lai, C. K.; Ke, Y. C.; Su, J. C.; Lu, C. S.; Li, W. R. *Liq. Cryst*. **2002**, *29*, 915.
(13) (a) Incarvito, C.; Rheingold, A. L.; Qin, C. J.; Gavrilova, A. L.; Bosnich, B. *Inorg. Chem*. **2001**, *40*, 1386. (b) Dong, Y. B.; Ma, J. P.; Huang, R. Q.; Smith, M. D.; Loye, H. C. *Inorg. Chem*. **2003**, *42*, 294. (c) Dong, Y. B.; Cheng, J. Y.; Huang, R. Q.; Smith, M. D.; Loye, H. C. *Inorg. Chem*. **2003**, *42*, 5699. (d) Richardson, C.; Steel, P. J.; D'Alessandro, D. M.; Junk, P. C.; Keene, F. R. *J. Chem. Soc., Dalton Trans*. **2002**, 2775. (e) da Silva, A. S.; de Silva, M. A. A.; Carvalho, C. E. M.; Antunes, O. A. C.; Herrera, J. O. M.; Brinn, I. M.; Mangrich, A. S. *Inorg. Chim. Acta* **1999**, *292*, 1.
(14) (a) El Kaim, L.; Le Menestrel, I.; Morgrntin, R. *Tetrahedron Lett.* **1998**, *39*, 6885. (b) Young, J. R.; DeVita, R. J. *Tetrahedron Lett.* **1998**, *39*, 3931. (c) Verheyde, B.; Dehaen, W. *J. Org. Chem*. **2001**, *66*, 4062.

Scheme 1

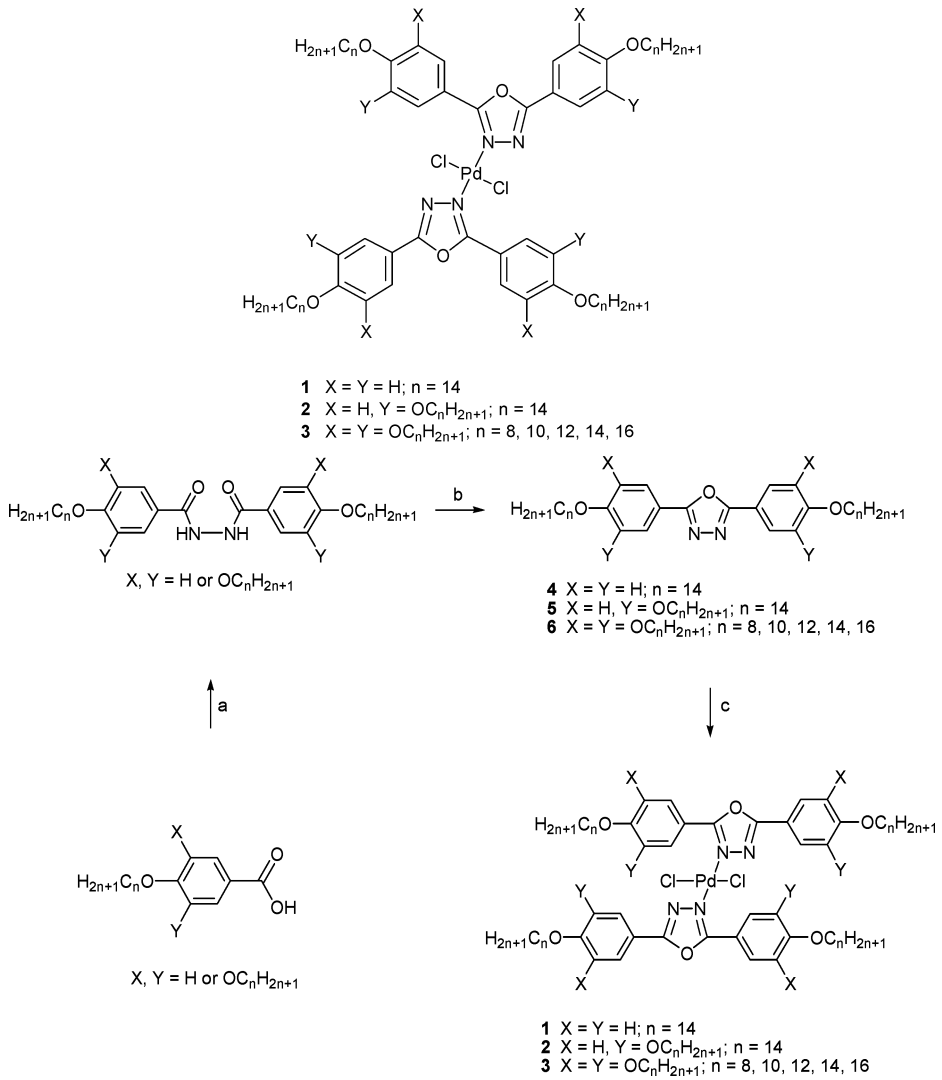

Reagents and conditions: a, refluxed in $SOCl_2$ 1 h, then $N_2H_4 \cdot H_2O$ (1.0 eq), stirred in THF 2 h, 78−92%; b, PCl_3 (10.0 equiv), refluxing in THF or toluene 4−8 h, 60−75%; c, $PdCl_2$ (0.55 equiv), refluxing in EtOH/H_2O (5:1) 24 h, 80−91%.

dium(II)-d^8 complexes are not air-sensitive and also quite stable. The mesomorphic behavior of the compounds **1**−**3** was studied by thermal analysis (DSC) and polarizing optical microscope. The phase transitions and thermodynamic data for compounds **1**−**3** are summarized in Table 1. As can be seen from the table, the formation of mesophases observed was strongly dependent on the numbers of flexible chains attached to the core group. All compounds **3** ($n \geq 8$) appended with twelve side chains exhibited columnar phase, however, the compounds **1** and **2** appended with four or eight chains formed crystalline. In contrast, a phase transition of crystal-to-isotropic at 163.7 °C and 120.2 °C was only observed for compound **1** and **2**, respectively. The lack of mesomorphic behavior observed by **1** and **2** was attributed to an insufficiency of side chain density for formation of a stable columnar phase. The formation of columnar phases was generally found to depend crucially on the side chain density, and most columnar mesogens or metallomesogens formed by discotic molecules[15,16] have at least eight side chains. The side chain density required for the columnar phases was strongly dependent on the core size, i.e., the larger the core center, the more side chain density is needed. In fact a few examples[17] of metallomesogenic structures with three side chains, which exhibited columnar phases have been reported. The molecules in this type of correlated columnar phase are generally organized with an antiparallel arrangement within the columns.

In contrast, all of the compounds **3** exhibited enantiotropic behavior regardless of the chains' length. The derivative with a shorter carbon length $n = 8$ is a yellow viscous paste in appearance at room temperature, and is truly mesognic at room temperature (RT). Its melting or crystallization tem-

(15) (a) Chandrasekhar, S. *Adv. Liq. Cryst.* **1982**, *5*, 47. (b) Destrade, C.; Foucher, P.; Gasparoux, H.; Nguyen, H. T.; Levelut, A. M.; Malthete, J. *Mol. Cryst. Liq. Cryst.* **1984**, *106*, 121. (c) Zheng, H. X.; Lai, C. K.; Swager, T. M. *Chem. Mater.* **1995**, *7*, 2067. (d) Takada, A.; Ide, N.; Fukuda, T.; Miyamoto, T.; Yamagata, K.; Watanabe, J. *Liq. Cryst.* **1995**, *19*, 441.

(16) (a) Szydlowska, J.; Krówezyński, A.; Górecka, E.; Pociecha, D. *Inorg. Chem.* **2000**, *39*, 4879. (b) Artzner, F.; Veber, M.; Clerc, M.; Levelut, A.-M. *Liq. Cryst.* **1997**, *23*, 27.

(17) (a) Kim, S. J.; Kang, S. H.; Park, K. M.; Zin, W. C.; Chio, M. G.; Kim, K. *Chem. Mater.* **1998**, *10*, 1889. (b) Coco, S.; Espinet, P.; Martin-Alvarez, A. J.; Levelut, A. M. *J. Mater. Chem.* **1997**, *7*, 19.

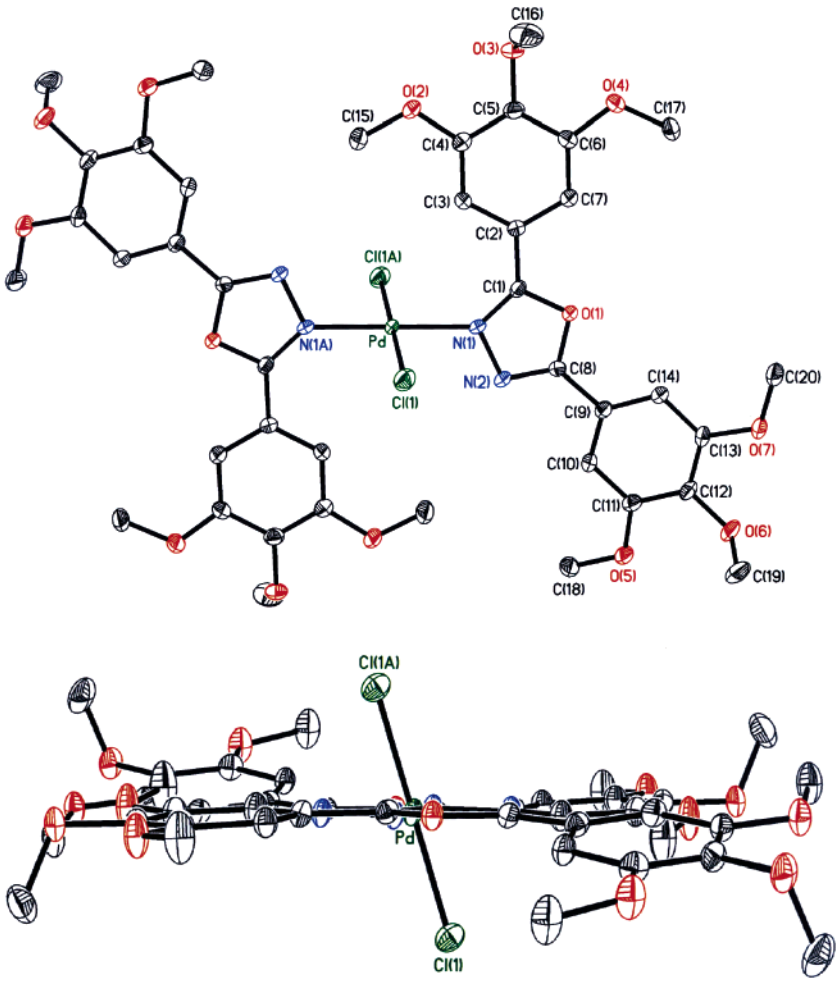

Figure 1. Two examples of ORTEP drawings for palladium complex with the numbering scheme, and the thermal ellipsoids of the non-hydrogen atoms drawn at the 50% probability level.

perature was not obtained at temperature cooled to −30 °C on DSC cycle. All other compounds **3** ($n > 8$) gave two typical transitions[18] of crystal-to-columnar and columnar-to-isotropic (K→Col→I) by DSC analysis. This type of phase behavior was typically observed for columnar or discotic molecules. All melting temperatures were in the range 0.86−51.4 °C, which increased with side chains length, i.e., 0.86 °C ($n = 10$) to 51.4 °C ($n = 16$). The transition temperature of mesophase-to-isotropic for the compounds was observed at 144.5−102.4 °C, and the clearing temperatures were decreased with increasing the carbon length of side chains. Therefore, the temperature range of mesophase was decreased with carbon chains length, i.e., 174.0 °C ($n = 8$) → 51.0 °C ($n = 16$) on heating cycle. Three derivatives with $n = 8$, 10, 12 were in fact room-temperature liquid crystals, and the derivative with $n = 8$ has the widest temperature (at least ca. 174.0 °C) of mesophase. In contrast, the derivative **3** ($n = 12$) has a melting point close to room temperature. Additionally, all transition enthalpies (8.52−1.15 kJ/mol) of columnar-to-isotropic were relatively lower than the transition enthalpies of crystal-to-columnar (19.7−27.5 kJ/mol) by DSC analysis, and this relatively small value of the transition enthalpy indicated that the mesophases were highly disordered. In addition, the magnitude of the $\Delta H_{Col\rightarrow I}$ was apparently decreased with the chains length, i.e. 8.52 kJ/mol ($n = 8$) →1.15 kJ/mol ($n = 16$), and this lowering in ΔH indicated that the disordering state or condition in the mesophase was increased as chains' length increases. Interestingly, a parameter ($x = \Delta H_{K\rightarrow Col}/\Delta H_{Col\rightarrow I}$) calculated by the enthalpy of two transitions was also estimated, and the x value was found to decrease with chain length, i.e. 19.7/3.71 = 5.31, 9.89, 12.2, to 23.2 for $n = 10$, 12, 14, and 16, respectively. Whether the increasing x value by the chain length correlates with columnar phase changed rectangular to hexagonal columnar phases observed in this system is uncertain at this moment. However, the x value might reflect or represent the relative disordering state of the two transition states.

The mesophase observed for the derivatives $n = 8$, 10, 12, 14 was identified as rectangular columnar (Col_r) based on optical textures observed under the optical microscope. A mosaic texture with prominent wedge-shaped defect or leaf-platelike under the polarized microscope was easily observed. On the other hand, as the carbon chains length increased to higher homologue ($n = 16$) a hexagonal

(18) (a) Lai, C. K.; Tsai, C. H.; Pang, Y. S. *J. Mater. Chem.* **1998**, *8*, 1355. (b) Ohta, K.; Azumane, S.; Kawahara, W.; Kobayashi, N.; Yamamoto, I. *J. Mater. Chem.* **1999**, *9*, 2313. (c) Heinrich, B.; Praefcke, K.; Guillon, D. *J. Mater. Chem.* **1997**, *7*, 1363. (d) Ohta, K.; Yamaguchi, N.; Yamamoto, I. *J. Mater. Chem.* **1998**, *8*, 2637. (e) Ban, K.; Nishizawa, K.; Ohta, K.; Shirai, H. *J. Mater. Chem.* **2000**, *10*, 1083.

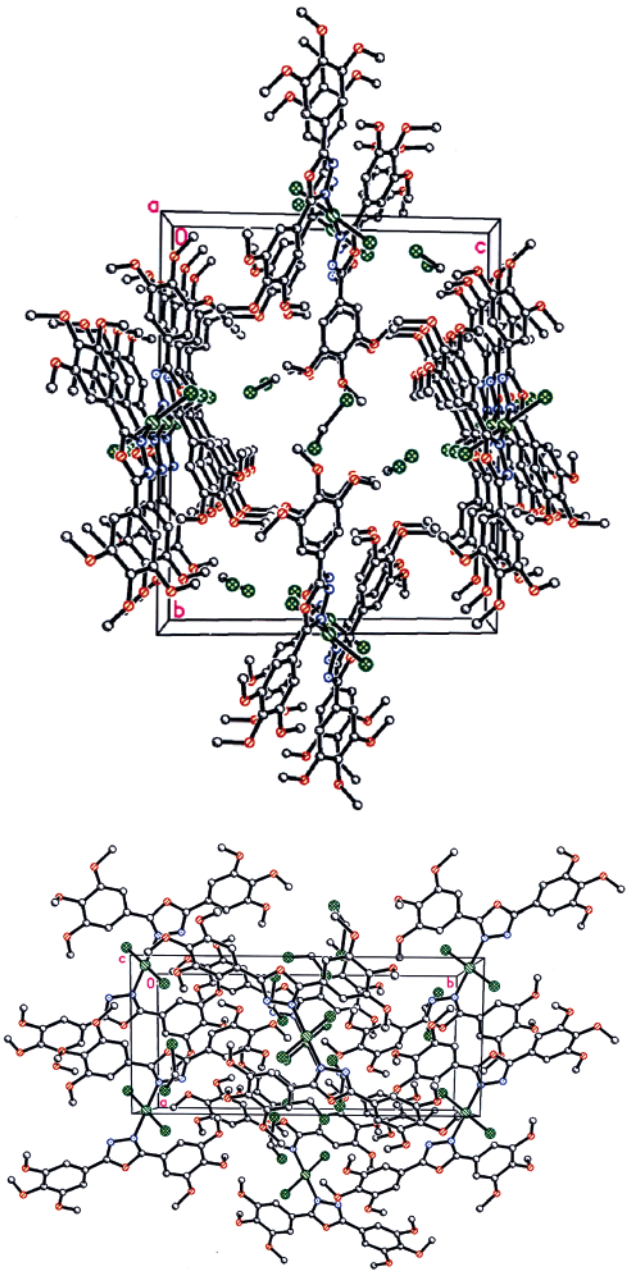

Figure 2. Two different views of the crystal packing approximately down the *b* axis and *a* axis.

columnar phase (Col_h) was then observed. In this case a typically pseudo focal-conic texture with linear birefrigent defects on slowly cooling from the isotropic liquid was clearly observed. This observed texture also accompanied by a large area of homeotropic domain is often characteristic for hexagonal columnar phases. Figure 3 shows the typical optical textures of Col_r and Col_h phases by **3** ($n = 8$ and 16). This type of columnar mesophase changing from rectangular to hexagonal columnar phases as carbon chain length increased was occasionally observed in other discotic systems.[15−16] A transition from a Col_r to Col_h superstructure resulted when the molecules projected an elliptical shape along the column's axis, and the molecules are generally tilted within the columns in such phase. Three types of symmetry of the Col_r phase are long known, $C(2/m)$, $P(2/a)$, and $P(2_1/b)$ depending on the structure of the molecules. An observation of the transition from a Col_r to Col_h phase

Table 1. Phase Behavior[a] for the Compounds 1−3

1	$n = 14$			K_1	155.0 (13.7) ⇌ 144.9 (2.33)	K_2	163.7 (14.0) ⇌ 151.8 (20.0)	I
2	$n = 14$			K_1	75.6 (7.79) ⇌ 67.7 (15.5)	K_2	120.2 (56.3) ⇌ 101.0 (57.1)	I
3	$n = 8$			K	< 30.0 °C ⇌ < 30.0 °C	Col_r	144.5 (8.52) ⇌ 135.5 (7.35)	I
	$n = 10$			K	0.86 (19.7) ⇌ −2.55 (18.0)	Col_r	125.9 (3.71) ⇌ 115.0 (3.37)	I
	$n = 12$	K_1	22.0 (13.0) ⇌ 14.7 (12.2)	K_2	25.3 (27.0) ⇌ 21.3 (27.4)	Col_r	118.1 (2.73) ⇌ 109.2 (2.47)	I
	$n = 14$	K_1	46.4 (24.9) ⇌ 39.8 (8.96)	K_2	48.2 (27.5) ⇌ 42.3 (21.8)	Col_r	113.1 (2.25) ⇌ 105.4 (2.23)	I
	$n = 16$	K_1	49.0 (33.5) ⇌ 37.5 (23.6)	K_2	51.4 (26.7) ⇌ 45.2 (36.3)	Col_h	102.4 (1.15) ⇌ 93.4 (1.04)	I

[a] *n* represents the number of carbons in the alkoxy chain. K_1, K_2= crystal phases; Col_h= hexagonal columnar phase; Col_r= rectangular columnar phase; I = isotropic. The transition temperatures (°C) and enthalpies (in parentheses, kJ/mol) are determined by DSC at a scan rate of 5.0 °C/min.

was often accomplished with longer side chains. In some cases, this type of $Col_r \rightarrow Col_h$ transition[16] occurred when temperature was raised.

The mesomorphic behavior observed by compounds **6** (ligands) and **3** (Pd^{2+} complexes) was also compared and the results are depicted in Figure 4. The clearing temperatures were increased by ca. 74.0 °C (for $n = 8$) to 48.3 °C (for $n = 16$) upon complexation to Pd^{2+} ion. The relative rigidity of the central core is generally increased due to a larger molecule or overall shape formed after coordination to the metal ions. In addition, the temperature range of columnar phases was much wider in **3** than **6** by ca. 140.0 °C ($n = 8$) to 45.0 °C ($n = 16$). The more kinetically stable mesophase indicated that an improved phase was produced or observed by a better discotic palladium compounds **3** over the nondiscotic ligand compounds **6**, i.e., a better aspect ratio was obtained after forming a round molecule.

Variable-temperature powder XRD diffraction was also used to confirm the structure of the columnar phases. A summary of the diffraction peaks and lattice for compounds **3** is listed in Table 2. For the derivatives with $n = 10$, 12, 14, two stronger and one weaker diffraction peaks at lower angle and one diffuse broad peak at wide-angle were typically observed. This type of diffraction pattern[18] corresponded to rectangular columnar arrangement (Col_r), and these peaks are corresponding to Miller indices (200), (110), and (310). For example, the derivative **3** ($n = 10$) gave a diffraction of two strong reflections at *d* 25.64 Å and 18.59 Å, a weaker peak at 12.95 Å, and also a broad diffuse peak at 4.38 Å at 70 °C. The two strong low-angle peaks are indexed as (200) and (110) and the third weaker peak at slightly higher angle is indexed as (310). This diffraction corresponded to a rectangular lattice constants of $a = 51.28$ Å and $b = 19.95$ Å. This lattice might seem to be too long and thin and the disk might incline very steeply to avoid forming a columnar arrangement. A similar lattice constant was observed in other columnar system.[18c] The possibility in forming a tetragonal columnar (Col_{tet}) structure was also considered and the

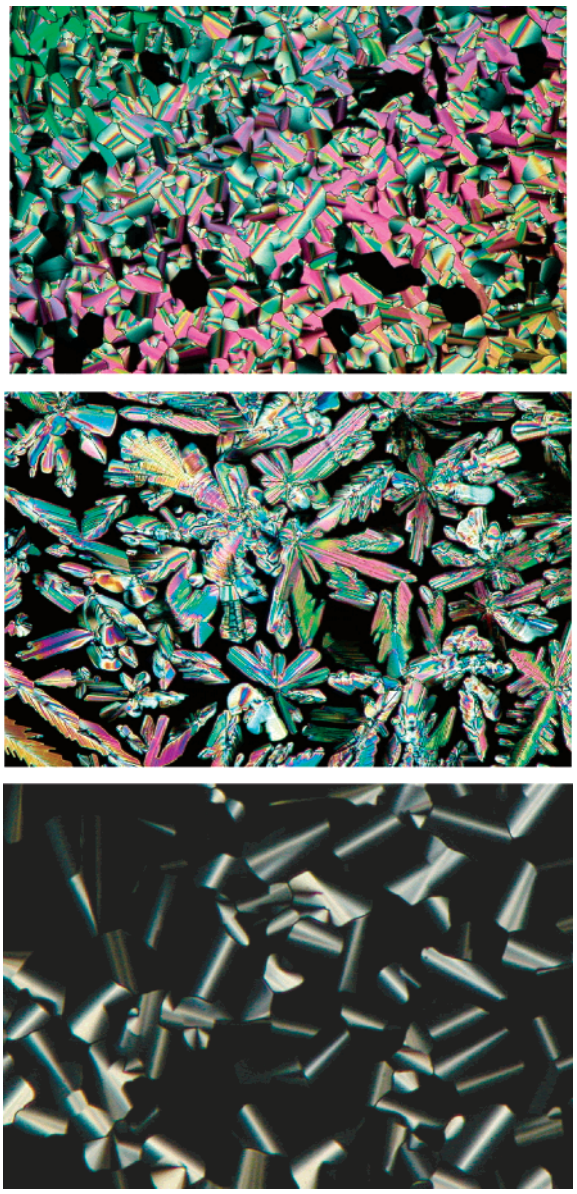

Figure 3. Optical textures observed: top, Col_h by **6** ($n = 8$) at 60 °C; middle, Col_r phase at 125.0 °C by **3** ($n = 8$); bottom, Col_h phase by **3** ($n = 16$) at 70 °C.

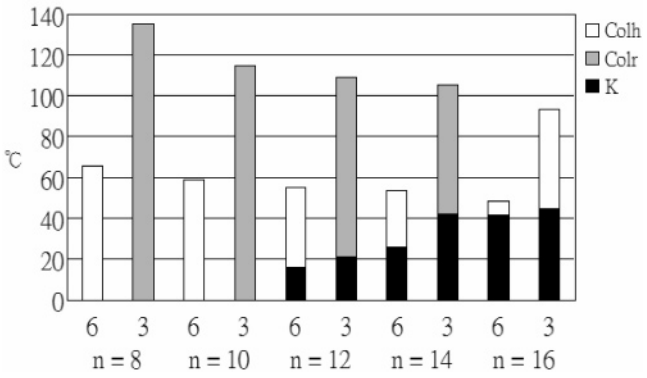

Figure 4. Bar graph showing the phase behavior of the ligands **6** and palladium complexes **3**; n = is the number of the alkoxy side chains.

spacing ratio of $1:(1/2)^{1/2}:1/2$ was used to fit all the diffraction peaks. However, the diffraction peaks were not well correlated as carbon length increased (especially for derivatives $n = 12$, 14). Therefore, the structure of columnar phases was tentatively assigned as Col_r phases. The reflection

Table 2. Powder XRD Diffraction Data of Palladium(II) Compounds 3

compd	n	mesophase	temp (°C)	lattice spacing (Å)	d-Spacing obs. (calcd) (Å)	Miller indices
3	10	Col_r	70	$a = 51.28$	25.64 (25.64)	(200)
				$b = 19.95$	18.59 (18.59)	(110)
					12.95 (12.98)	(310)
					4.38 (br)	(halo)
	12	Col_r	70	$a = 54.88$	27.44 (27.44))	(200)
				$b = 22.09$	20.49 (20.49)	(110)
					14.05 (14.09)	(310)
					4.42 (br)	(halo)
	14	Col_r	70	$a = 58.46$	29.23 (29.23)	(200)
				$b = 24.28$	22.42 (22.42)	(110)
					15.14 (15.20)	(310)
					4.46 (br)	(halo)
	16	Col_h	60	$a = 63.43$	54.93 (54.93)	(100)
					31.69 (31.71)	(110)
					27.47 (27.47)	(200)
					4.57 (br)	(halo)

d-spacings of all derivatives were also correlated well with increasing carbon chains length, i.e., 25.64 Å, 18.59 Å ($n = 10$); 27.44 Å, 20.49 Å ($n = 12$); 29.23 Å, 22.42 Å ($n = 14$). However, the powder XRD diffraction pattern for derivatives $n = 16$ was apparently different, which was also consistent with the textures observed by optical microscope. A diffraction pattern of an intense peak at 54.93 Å, 31.69 Å, and 27.47 Å and a broad diffuse peak (4.57 Å) at wide-angle region was observed and this diffraction pattern corresponded to a hexagonal columnar arrangement. This pattern corresponds to an intercolumnar distance of 63.43 Å. In both Col_h and Col_r arrangements the absence of any distinct peak at higher angle (at d 3.3−3.5 Å) precluded the observed columnar structures (Col_{ho} or Col_{ro}) from a more regular

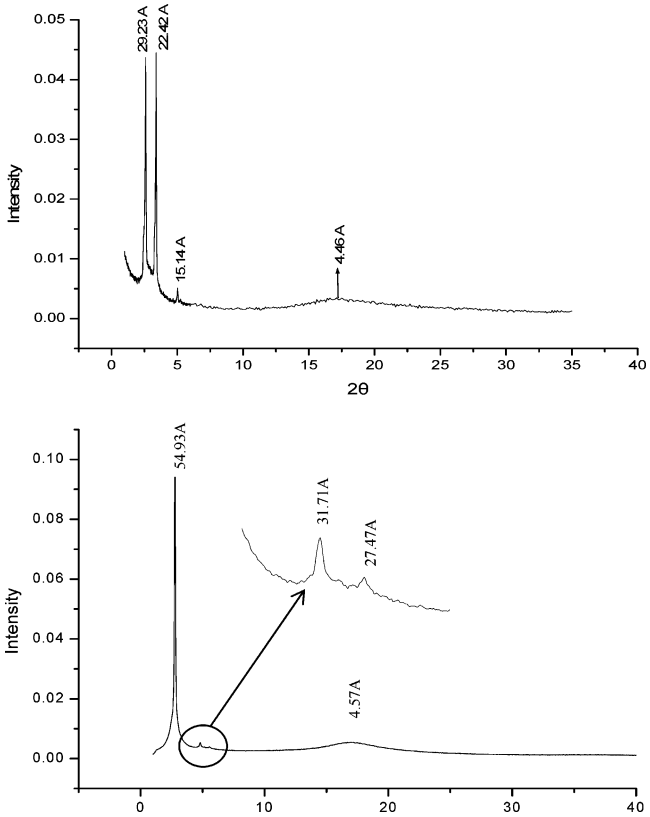

Figure 5. X-ray diffraction data of the palladium compounds **3**: Col_r phase at 70 °C ($n = 14$, top) and Col_h phase at 60 °C ($n = 16$, bottom).

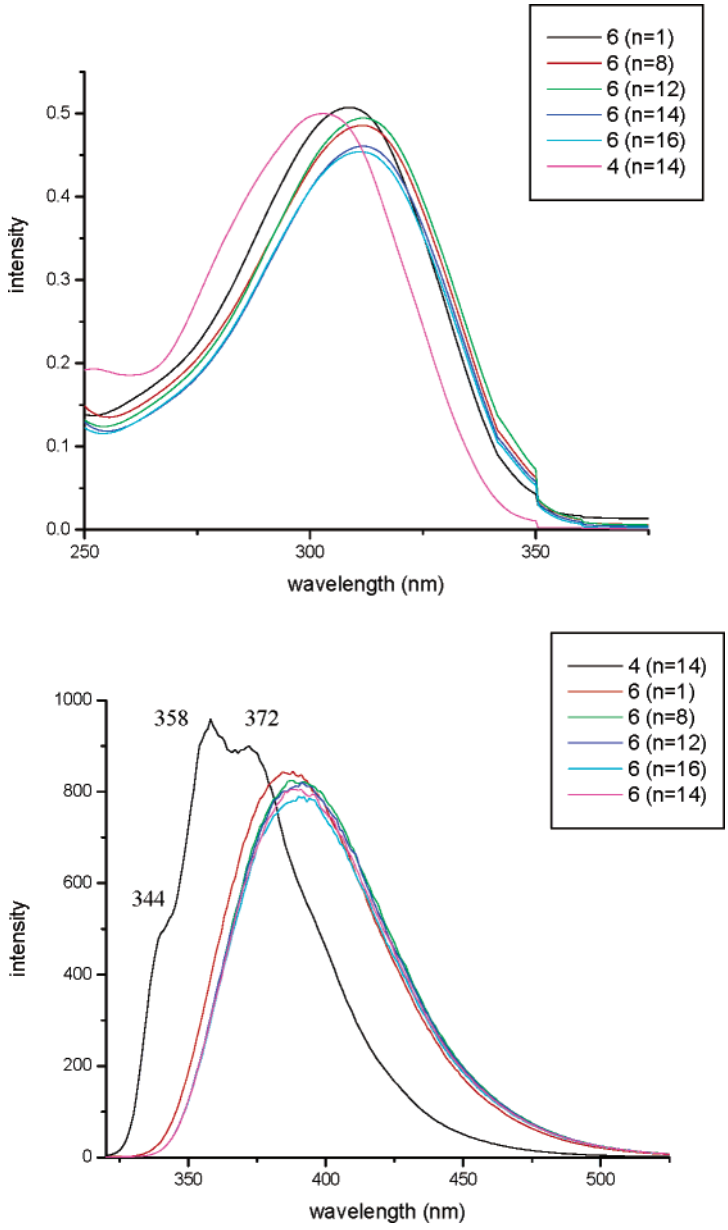

Figure 6. Normalized UV (top) and PL (bottom) spectra of compounds **4** and **6** in CH_2Cl_2 at room temperature.

periodicity along the columns. These data were also quite consistent with the relatively small transition enthalpies of columnar-to-isotropic obtained by DSC analysis. A typical example of a diffraction pattern for Col_h ($n = 16$) and Col_r ($n = 14$) phases was depicted in Figure 5. The pseudo-hexagonal lattice constant,[18,19] which is a rectangular lattice with an axial ratio of an ideal hexagon of $3^{1/2}$ (as shown in Scheme 2) was also calculated, and this constant ranged from $a/b = 2.57$ (i.e., 51.28/19.95 for $n = 10$) to 2.41 ($n = 14$). These values indicated that the structural departure from an ideal hexagonal lattice were roughly about 25.7−2.41%. On the other hand, the dependence on decreasing a/b value with side chain lengths also indicates a greater anisotropy or more elliptical exhibited by shorter side chains over longer side chains along the columnar axis.

Optical Properties. 1,3,4-Oxadiazole derivatives have been studied due to their photophysical and fluorescent properties. The UV−vis absorption spectra for compounds **4** and **6** in CH_2Cl_2 solution are presented in Figure 6. All compounds exhibited a unique intense broad absorption peak at 303−312 nm, and these absorption spectra were very similar in shape because of their structural similarity. The highest absorption peaks of all compounds were insensitive to the carbon length and numbers of terminal chains, and they all occurred at ca. 303 nm for **4** and 309−312 nm for **6**. The data of λ_{max} peaks are listed in Table 3. Increasing

Scheme 2. Correlation between Lattice Constants *a* and *b* Values in Col_h and Col_r Arrangements

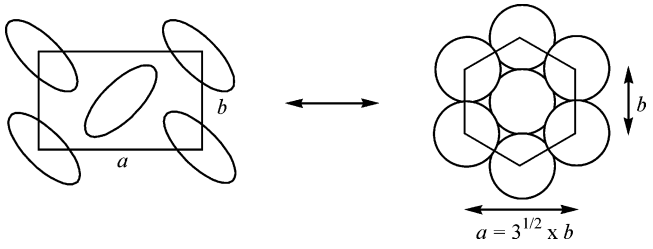

(19) Heinrich, B.; Praefcke, K.; Guillon, D. *J. Mater. Chem.* **1997**, *7*, 1363.

Table 3. Photophysical Properties of Compounds 4 and 6[a]

compd	*n*	λ_{max} abs/nm	λ_{max} EM/nm	Φ
4	14	303	358, 372	0.0010
6	1	309	388	0.0011
	8	312	388	0.00138
	12	312	391	0.00137
	14	312	391	0.00134
	16	311	390	0.00132

[a] Spectra measured in CH_2Cl_2 at room temperature.

the numbers of electron-donating alkoxy groups (**4**→**6**) showed slightly red shift by ca. 9.0 nm. The derivative with shorter carbon length (**6**, $n = 1$) has the λ_{max} peak lower than that of the derivative with longer carbon length (**6**, $n = 16$) by ca. 3.0 nm. The emission luminescence spectra measured in CH_2Cl_2 of compounds **4**−**6** are also shown in Figure 6. A similar trend was also observed in the photoluminescence spectra. The emission peaks occurred at 358−391 nm. The solution PL spectra peak shapes were quite similar to those of the UV−vis spectra except for compound **4** ($n = 14$). This compound has a more complex spectrum than others both in spectra shape and λ_{max}, and exhibits two λ_{max} at 358 and 372 nm and a broad shoulder at lower 344 nm. Increasing the electron-donating OR groups led to a slight red shift of λ_{max} by ca. 33 nm (i.e., 391−358 nm). However, the quantum yields of all compounds in CH_2Cl_2 estimated with anthracene as a standard ($\varphi_f = 0.27$ in hexane) were relatively low, and were in the range 0.10%−0.13%.

Conclusions

A new series of palladium(II) complexes based on heterocyclic 1,3,4-oxadiazole as core group were prepared, and some of these compounds are room-temperature liquid crystals. All palladium(II) complexes exhibited a better or improved mesomorphic behavior (i.e., a wider range of mesophase temperature) than the unchelated ligand derivatives. A single-crystal analysis was resolved and used to understand the relationship of the structure and the observed phases. The distance estimated between the two molecules in columns of ca. 4.161 Å was slightly longer than the 3.3−3.5 Å normally found in other discotic systems, and this longer packing distance led to a weaker interaction within the columnar direction. Therefore, the two *trans*-chlorine atoms located perpendicular to the molecular plane might be attributed to a melting temperature lower than that observed in other similar systems.

Experimental Section

General. All chemicals and solvents were reagent grade from Aldrich Chemical Co. Toluene and dichloromethane were dried by standard technique. ^{1}H and ^{13}C NMR spectra were measured on a Bruker DRS-200. DSC thermographs were carried out on a Mettler DSC 822 and calibrated with a pure indium sample. All phase transitions are determined by a scan rate of 5.0°/min. Optical polarized microscopy was carried out on Zeiss Axioplan 2 equipped with a hot stage system of Mettler FP90/FP82HT. The UV−vis absorption and fluorescence spectra were obtained using a Hitachi F-4500 or Jasco V-530 spectrometer, and all spectra were recorded at room temperature. Elemental analyses for carbon, hydrogen, and nitrogen were conducted at Instrumentation Center, National Taiwan University on a Heraeus CHN-O-Rapid elemental analyzer. The data are summarized in Table 4. Data for all X-ray structures were collected using a Bruker Smart CCD diffractometer with graphite-monochromated Mo Kα radiation ($\lambda = 0.71073$ Å) at 150 ± 1 K. The structure was solved by direct methods and refined by full matrix least-squares and difference Fourier techniques with SHELXTL. Empirical absorption corrections were applied with SADABS program. All non-hydrogen atoms were refined anisotropically. The powder diffraction data were collected from the Wiggler-A beamline of the National Synchrotron Radiation Research Center (NSRRC) with the wavelength of 1.3263 Å. Diffraction patterns were recorded in $\theta/2\theta$ geometry with step scans normally 0.02° in $2\theta = 1-10°$ step^{-1} s^{-1} and 0.05° in $2\theta = 10-25°$ step^{-1} s^{-1} and a gas flow heater was used to control the temperature. The powder samples were charged in Lindemann capillary tubes (80 mm long and 0.01 mm thick) from Charles Supper Co. with an inner diameter of 1.0 or 1.5 mm. Known compounds such as 4-alkoxy-, 3,4-dialkoxy-, and 3,4,5-trialkoxybenzoic acids, 4-alkoxy-, 3,4-dialkoxy-, and 3,4,5-alkoxy benzoic acid, and *N*-(3,4,5-trialkoxybenzoyl)hydrazides[12,18] were followed by previously published procedures.

Table 4. Elemental Analysis[a] (%) of Compounds 1−3

compd	*n*	C	H	N
1	14	68.92 (68.57)	9.30 (9.04)	3.43 (3.81)
2	14	72.85 (72.45)	11.00 (10.60)	2.16 (2.41)
3	8	68.38 (68.94)	10.10 (9.89)	2.72 (2.59)
	10	70.84 (71.19)	10.92 (10.50)	2.23 (2.24)
	12	71.31 (72.90)	11.48 (10.96)	1.42 (1.98)
	14	74.45 (74.26)	11.78 (11.32)	1.63 (1.77)
	16	75.45 (75.35)	12.26 (11.61)	1.38 (1.60)

[a] With calculated values in parentheses.

3,4,5-Tritetradecanoxybenzoic Acid (n = 14). White solids, yield 91%. ^{1}H NMR ($CDCl_3$): δ 0.86 (m, $-CH_3$, 9H), 1.16−1.81 (m, $-CH_2$, 72H), 4.00 (m, $-OCH_3$, 6H), 7.36 (s, $-C_6H_2$, 2H). ^{13}C NMR ($CDCl_3$): δ 14.09, 22.68, 26.05, 29.37, 29.61, 30.30, 31.91, 69.07, 73.49, 108.39, 123.66, 143.00, 152.77, 172.21.

3,4-Ditetradecanoxybenzoic Acid (n = 14). White solids, yield 92%. ^{1}H NMR ($CDCl_3$): δ 0.88 (m, $-CH_3$, 9H), 1.29−1.83 (m, $-CH_2$, 48H), 4.04 (m, $-OCH_2$, 4H), 6.88 (d, $J = 8.52$ Hz, $-C_6H_3$, 1H), 7.61−7.74 (m, $-C_6H_3$, 2H). ^{13}C NMR ($CDCl_3$): δ 14.03, 22.68, 26.05, 29.24, 29.35, 29.60, 31.95, 69.32, 69.64, 112.50, 115.41, 121.80, 124.64, 148.93, 154.34, 171.83.

4-Tetradecanoxybenzoic Acid (n = 14). White solids, yield 95%. ^{1}H NMR ($CDCl_3$): δ 0.86 (t, $J = 6.00$ Hz, $-CH_3$, 3H), 1.23−1.83 (m, $-CH_2$, 24H), 3.93 (t, $J = 6.49$ Hz, $-OCH_2$, 2H,), 6.98 (d, $J = 8.84$ Hz, $-C_6H_4$, 2H), 8.02 (d, $J = 8.81$ Hz, $-C_6H_4$, 2H). ^{13}C NMR ($CDCl_3$): δ 14.03, 22.61, 25.91, 29.04, 29.29, 29.61, 31.85, 68.71, 114.09, 126.03, 129.69, 162.33, 171.82.

3,4,5-Tritetradecanoxybenzoic Acid N-(3, 4, 5-tritetradecanoxybenzoyl)hydrazide (n = 14). White solids, yield 85%. ^{1}H NMR ($CDCl_3$): δ 0.87 (m, $-CH_3$, 18H), 1.23−1.44 (m, $-CH_2$, 132H), 1.71−1.75 (m, $-CH_2$, 12H), 3.98 (m, $-OCH_2$, 12H), 7.05 (s, $-C_6H_2$, 4H), 9.73 (br, −NH, 2H). ^{13}C NMR ($CDCl_3$): δ 14.07, 22.68, 26.11, 29.37, 29.49, 29.69, 30.37, 31.93, 69.14, 73.44, 105.66, 125.78, 141.71, 153.14, 165.29.

3,4-Ditetradecanoxybenzoic Acid N-(3,4-ditetradecanoxybenzoyl)-hydrazide (n = 14). White solids, yield 94%. ^{1}H NMR ($CDCl_3$): δ 0.87 (m, $-CH_3$, 12H), 1.23−1.45 (m, $-CH_2$, 88H), 1.71−1.87 (m, $-CH_2$, 8H), 4.00 (m, $-OCH_2$, 8H), 6.83 (d, $J = 8.90$ Hz, $-C_6H_3$, 2H), 7.40 (m, $-C_6H_3$, 4H), 9.38 (br, −NH, 2H). ^{13}C NMR ($CDCl_3$): δ 13.74, 22.41, 25.83, 29.03, 29.10, 29.18, 29.21, 29.38, 29.41, 29.46, 31.69, 69.14, 69.38, 112.69, 112.88, 120.38, 123.78, 149.14, 152.79, 164.27.

4-Tetradecanoxybenzoic Acid N-(4-tetradecanoxybenzoyl)hydrazide (n = 14). White solids, yield 86%. ^{1}H NMR ($CDCl_3$): δ 0.88 (m, $-CH_3$, 6H), 1.23−1.44 (m, $-CH_2$, 44H), 1.72−1.82 (m, $-CH_2$, 4H), 4.02 (m, $-OCH_2$, 4H), 6.87 (d, $-C_6H_4$, 4H, J = 8.00 Hz), 7.80 (d, J = 8.20 Hz, $-C_6H_4$, 4H), 9.21 (b, −NH, 2H). ^{13}C NMR ($CDCl_3$): δ 13.97, 22.64, 26.04, 29.21, 29.31, 29.38, 29.63, 31.92, 68.43, 114.60, 123.84, 129.23, 162.62, 164.44.

*2,5-Bis(3,4,5-tritetradecanoxyphenyl)-1,3,4-oxadiazole (**6**; n = 14).* Dry toluene solution (30.0 mL) of 3,4,5-tridecanoxybenzoic acid *N*-(3, 4, 5-tritetradecanoxybenzoyl) hydrazide (3.00 g, 0.002 mol) was slowly added to phosphorus chloride (3.0 g, 0.022 mol), and the solution was gently refluxed for 8 h under nitrogen atmosphere. The solution was concentrated to give brown solids and the residue was purified by chromatography (Al_2O_3; CH_2Cl_2/hexane, 1:1). White solids were obtained after recrystallization from CH_2Cl_2/CH_3OH. Yield 70%. ^{1}H NMR ($CDCl_3$): δ 0.86 (m, $-CH_3$, 18H), 1.20−1.56 (m, $-CH_2$, 132H), 1.72−1.86 (m, $-CH_2$, 12H), 4.06 (m, $-OCH_2$, 12H), 7.29 (s, $-C_6H_2$, 4H). ^{13}C NMR ($CDCl_3$): δ 14.01, 22.65, 26.12, 29.34, 29.43, 29.46, 29.58, 29.65, 29.71, 30.39, 31.93, 69.77, 73.69, 106.20, 118.71, 141.93, 153.70, 164.60. IR (KBr): 733, 841, 992, 1118, 1209, 1241, 1339, 1379, 1432, 1467, 1492, 1557, 1591, 2854, 2924, 2955 cm^{-1}.

*2,5-Bis(3,4-ditetradecanoxyphenyl)-1,3,4-oxadiazole (**5**; n = 14).* White solids, yield 68%. ^{1}H NMR ($CDCl_3$): δ 0.85 (m, $-CH_3$, 12H), 1.21−1.42 (m, $-CH_2$, 88H), 1.70−1.80 (m, $-CH_2$, 8H), 4.04 (q, J = 6.66 Hz, $-OCH_2$, 8H), 6.87 (d, J = 8.98 Hz, $-C_6H_3$, 2H), 7.51−7.56 (m, $-C_6H_3$, 4H). ^{13}C NMR ($CDCl_3$): δ 13.94, 22.60, 26.01, 26.03, 29.27, 29.35, 29.53, 29.57, 31.87, 69.41, 69.77, 112.50, 113.61, 116.81, 120.43, 149.67, 152.44, 164.28. IR (KBr): 722, 1107, 1144, 1228, 1277, 1378, 1466, 1499, 1736, 2850, 2918, 2955 cm^{-1}.

*2,5-Bis(4-tetradecanoxyphenyl)-1,3,4-oxadiazole (**4**; n = 14).* White solids, yield 70%. ^{1}H NMR ($CDCl_3$): δ 0.86 (t, J = 6.05 Hz, $-CH_3$, 6H), 1.26−1.45 (m, $-CH_2$, 44H), 1.73−1.86 (m, $-CH_2$, 4H), 4.01 (t, J = 6.47 Hz, $-OCH_2$, 4H), 6.99 (d, J = 8.83 Hz, $-C_6H_4$, 4H,), 8.02 (d, J = 8.82 Hz, $-C_6H_4$, 4H). ^{13}C NMR ($CDCl_3$): δ 14.00, 22.66, 26.05, 29.22, 29.34, 29.38, 29.58, 29.69, 31.93, 68.44, 114.67, 115.12, 116.70, 128.59, 161.96, 164.19. IR (KBr): 742, 836, 1175, 1257, 1300, 1377, 1469, 1496, 1611, 1731, 2851, 2915 cm^{-1}.

*Dichlorobis[2,5-bis(3,4,5-tritetradecanoxyphenyl)-1,3,4-oxadiazole]palladium(II) (**3**; n = 14).* 2,5-Bis(3,4,5-tritetradecanoxyphenyl)-1,3,4-oxadiazole (0.50 g, 0.00033 mol) was dissolved in hot EtOH/THF (10:1, 40 mL), and to the solution palladium(II) chloride dissolved in EtOH/H_2O (5:1; 10 mL) was then added. The reaction mixture was refluxed for 24 h. Yellow solids were filtered off, and the solids were rinsed several times with ethanol. The products isolated as yellow solids were obtained after recrystallization from CH_2Cl_2/CH_3OH. Yield 86%. IR (KBr): 721, 729, 797, 840, 881, 993, 1057, 1121, 1211, 1239, 1339, 1389, 1433, 1468, 1492, 1556, 1594, 2851, 2919, 2954 cm^{-1}. Anal. Calcd for $C_{196}H_{356}Cl_2N_4O_{14}Pd$: C, 74.26; H, 11.32; N, 1.77. Found: C, 74.45; H, 11.78; N, 1.63.

*Dichlorobis[2,5-bis(3,4-ditetradecanoxyphenyl)-1,3,4-oxadiazole]palladium(II) (**2**; n = 14).* Yellow solids, yield 81%. IR (KBr): 722, 1058, 1107, 1144, 1228, 1277, 1378, 1466, 1499, 1736, 2850, 2918, 2955 cm^{-1}. Anal. Calcd for $C_{140}H_{244}Cl_2N_4O_{10}Pd$: C, 72.45; H, 10.60; N, 2.41. Found: C, 72.85; H, 11.00; N, 2.16.

*Dichlorobis[2,5-bis(4-tetradecanoxyphenyl)-1,3,4-oxadiazole]palladium(II) (**1**; n = 14).* Yellow solids, yield 76%. IR (KBr): 742, 836, 1054, 1175, 1257, 1300, 1377, 1469, 1496, 1611, 1731, 2851, 2915, 2956 cm^{-1}. Anal. Calcd for $C_{84}H_{132}Cl_2N_4O_6Pd$: C, 68.57; H, 9.04; N, 3.81. Found: C, 68.92; H, 9.60; N, 3.43.

*Dichlorobis[2,5-bis(3,4,5-trioctanoxyphenyl)-1,3,4-oxadiazole]palladium(II) (**3**; n = 8).* Yellow paste, yield 79%. Anal. Calcd for $C_{124}H_{212}Cl_2N_4O_{14}Pd$: C, 68.94; H, 9.89; N 2.59. Found: C, 68.38; H, 10.10; N, 2.72. IR (KBr): 733, 842, 994, 1053, 1117, 1209, 1240, 1339, 1387, 1432, 1468, 1492, 1557, 1592, 2855, 2926, 2956 cm^{-1}.

*Dichlorobis[2,5-bis(3,4,5-tridecanoxyphenyl)-1,3,4-oxadiazole]palladium(II) (**3**; n = 10).* Yellow paste, yield 74%. Anal. Calcd for $C_{148}H_{260}Cl_2N_4O_{14}Pd$: C, 71.19; H, 10.50; N, 2.24. Found: C, 70.84; H, 10.92; N, 2.23. IR (KBr): 733, 841, 992, 1053, 1118, 1209, 1241, 1339, 1379, 1432, 1467, 1492, 1557, 1591, 2854, 2924, 2955 cm^{-1}.

*Dichlorobis[2,5-bis(3,4,5-tridodecanoxyphenyl)-1,3,4-oxadiazole]palladium(II) (**3**; n = 12).* Yellow solids, yield 88%. Anal. Calcd for $C_{172}H_{308}Cl_2N_4O_{14}Pd$: C, 72.90; H, 10.96; N, 1.98. Found: C, 72.31; H, 11.48; N, 1.42. IR (KBr): 733, 799, 842, 882, 999, 1052, 1118, 1209, 1240, 1288, 1339, 1379, 1433, 1468, 1492, 1557, 1592, 2853, 2923, 2957 cm^{-1}.

*Dichlorobis[2,5-bis(3,4,5-trihexadecanoxyphenyl)-1,3,4-oxadiazole]palladium(II) (**3**; n = 16).* Yellow solids, yield 88%. Anal. Calcd for $C_{220}H_{404}Cl_2N_4O_{14}Pd$: C, 75.35; H, 11.61; N, 1.60. Found: C, 75.45; H, 12.26; N, 1.08. IR (KBr): 721, 840, 988, 1051, 1121, 1239, 1340, 1388, 1443, 1468, 1492, 1555, 1593, 2850, 2918, 2954 cm^{-1}.

Acknowledgment. We thank the National Science Council of Taiwan, ROC and the UST for funding (NSC-92-2113-M-008-011) in generous support of this work.

Supporting Information Available: Crystallographic data and structure refinement for palladium complex of 2,5-bis(3,4,5-trimethoxyphenyl)-1,3,4-oxadiazole, selected bond distances for Pd complex, and DSC and TGA thermographs of **3** (pdf), and crystallographic information files for the subject compounds (cif). This material is available free of charge via the Internet at http://pubs.acs.org.

CM0483691